PHYSICAL REVIEW C VOLUME 16, NUMBER 3 SEPTEMBER 1977

Deformed-quasiparticle basis for calculating potential energy surfaces and nuclear spectra*

Krishna Kumar†
Physics Department, Vanderbilt University, Nashville, Tennessee

B. Remaud‡
Institut de Physique, Université de Nantes, Nantes, France

P. Aguer
Laboratoire S. Rosenblum du C.S.N.S.M., Orsay, France

J. S. Vaagen
NORDITA, Copenhagen, Denmark

A. C. Rester
Tennessee Technological University, Cookeville, Tennessee

R. Foucher
Institut de Physique Nucléaire, Orsay, France

J. H. Hamilton
Physics Department, Vanderbilt University, Nashville, Tennessee
(Received 28 December 1976)

The Nilsson model is combined with the Hill-Wheeler definition of nuclear deformations and with the stationarity condition of Yariv *et al.* to calculate a new deformed basis. The wave functions of this basis are the same for neutrons and for protons, and for all mass numbers. The energy levels depend on Z,A via an isospin-A-dependent scaling factor. This basis is combined with an improved theory of pairing to calculate a new deformed-quasiparticle basis. It is shown that without any adjustment of the model parameters from one nucleus to another, this basis leads to reasonable potential energy surfaces for many even-even nuclei (Mg,Zr,Sm,Er,Os,Hg), and reasonable low energy spectra of $^{24}_{12}$Mg, $^{102}_{40}$Zr, and $^{168}_{68}$Er. The Strutinsky method is used to calculate the potential energy surfaces. A modified Kumar-Baranger method is used to calculate the moments of inertia and the mass parameters, and to solve the collective Schrödinger equation.

[NUCLEAR STRUCTURE ^{148,150,152,154}Sm, ^{186,188,190,192,194}Os, ^{184,186,188,190}Hg; calculated deformation energy curves. ^{24}Mg, ^{102}Zr, ^{168}Er; calculated deformation energy curves and collective spectra. Modified Nilsson method. Modified BCS method. Combined Strutinsky method with Kumar-Baranger method.]

I. INTRODUCTION

In recent years, much progress has been made in calculating the potential energy surfaces of nuclear deformation. It is now generally recognized that the Strutinsky method[1] is a reliable simplification (computation time is reduced by several orders of magnitude) of the Hartree-Fock method of calculating the potential energy surfaces (see e.g., Refs. 2–4). Even then, the computation time is substantial.

Furthermore, it has been shown[5–7] that the potential energy is not enough for a complete description of nuclear spectra. It is necessary to calculate the dynamics of nuclear deformations, that is to solve the collective Schrödinger equation. In order to solve this equation, one needs to calculate not only the potential energy but also the moments of inertia and the mass parameters. An essential part of this method is the calculation of the potential and inertial functions not only as functions of β (magnitude of nuclear deformation) but also as functions of γ (the nonaxiality parameter).

Previous experience with calculations of this type has shown that most of the computation time is spent in the calculation of the single-particle basis (wave functions and matrix elements of various single-particle operators). Therefore, we have spent a number of years searching for a more efficient (less time consuming) basis which is at the same time reasonably complete. The purpose of this paper is to discuss a new single-particle basis which we have obtained recently. The main features of this basis are the following:

(1) All oscillator shells with $\mathfrak{N}=0$ to 8 are in-

cluded. Mixings of type $\Delta\mathfrak{N}=2$ and $\Delta\Omega=2$ (for nonaxial shapes) are taken into account exactly.

(2) The Nilsson[8] potential is combined with the Hill-Wheeler[9] (instead of Bohr-Mottelson[5,10]) definition of nuclear deformations.

(3) Strengths of the l^2 and $\vec{l}\cdot\vec{s}$ terms are assumed to be shell ($\mathfrak{N}$)-dependent rather than Z-A-dependent (except for an overall scaling factor for the energy levels). The same values are employed for protons and neutrons. Values for the lower shells ($\mathfrak{N}=0-2$) are determined by fitting the spectra of nuclei near closed shells. Those for the other shells are determined via a modified form of a stationarity condition due to Yariv, Ledergerber, and Pauli.[11]

(4) Our single-particle basis is independent of Z and A. Because of our exact treatment of $\Delta\mathfrak{N}=2$ mixing and $\Delta\Omega=2$ mixing in a large configuration space, we need to compute about six million matrix elements of various single-particle operators. However, the same matrix elements are employed for nuclei ranging from $A=24$ to $A=200$. Details are given in Sec. II.

After having calculated the deformed-single-particle basis, the next step in the present type of calculation is the inclusion of pairing, i.e., the calculation of the deformed-quasiparticle (DQP) basis. For this purpose we employ a modified BCS method. Our modification consists of including not only the particle-particle but also the particle-hole contributions of the pairing force. The major effect is to remove the divergence occurring in the BCS theory when two levels cross at the Fermi surface and the energy gap vanishes (quasiparticle energy, which appears in the denominator of many expressions, vanishes). Details are given in Sec. III.

How good is this DQP basis? We employ two types of tests. The first test is based on the question: Does the potential energy of nuclear deformation give the correct variations in regions of shape transitions? Using the Strutinsky method, we calculate the potential energy for a region of spherical-deformed transition ($^{148,\,150,\,152,\,154}_{62}$Sm), a region of prolate-oblate transition ($^{186,\,188,\,190,\,192,\,194}_{76}$Os), and a region of shape as well as energy gap transition ($^{184,\,186,\,188,\,190}_{80}$Hg). Details are given in Sec. IV.

The second test is based on the question: Is our DQP basis good enough for predicting the low-energy spectra of even-even nuclei without any adjustment of parameters from nucleus to nucleus? Of course, the answer depends not only on the DQP basis but also on the method of calculating the spectra. We employ the Strutinsky method of calculating the potential energy, and the modified Kumar-Baranger method of calculating the dynamics, i.e., calculating the moments of intertia and the mass parameters, and then solving the collective Schrödinger equation. Details are given in Sec. V.

The answer to the two questions mentioned above is a qualified yes. Without any adjustment of parameters from nucleus to nucleus, we do get reasonable potential energy surfaces for the nuclei mentioned above, and reasonable spectra for three test nuclei: $^{24}_{12}$Mg, $^{102}_{40}$Zr, and $^{168}_{68}$Er.

Reason for the qualification is the following. Although the dynamic theory employed here has previously been shown to be applicable to transitional nuclei like those of the osmium region[7] and those of the samarium region,[12] the present version of the model is valid only for the spectra of well-deformed nuclei. It is argued in Sec. VI that this is not the fault of either the DQP basis or that of the method of calculation of the potential and inertial functions. It is suggested that the fault lies in the neglect of the Villars-Cooper[13] correction which would give rotation-particle-coupling type of terms even for even-even nuclei (see the textbook by de-Shalit and Feshbach[14] for a beautiful discussion of this point).

Recently, this type of dynamic calculation in a large configuration space has also been performed by Dobaczewski, Rohozinski, and Srebrny.[15] They are able to get reasonable fits to transitional nuclei—but at the cost of introducing some *ad hoc* adjustments to the microscopically calculated potential and intertial functions. More comparison with their work is given in Sec. VI, which also gives our main conclusions.

II. DEFORMED-SINGLE-PARTICLE BASIS

The motion of a single nucleon in the field of the remaining $(A-1)$ nucleons is described in the Nilsson model via the Hamiltonian[8,10,16]

$$H_{\rm sv}=\vec{p}^2/(2M)+\tfrac{1}{2}M(\omega_1^2x_1^2+\omega_2^2x_2^2+\omega_3^2x_3^2)+\hbar\omega_0[v_{ll}(\vec{l}^2-\langle\vec{l}^2\rangle_N)+v_{ls}\vec{l}\cdot\vec{s}] \tag{1a}$$

$$\langle\vec{l}^2\rangle_N=\tfrac{1}{2}\mathfrak{N}(\mathfrak{N}+3)\,. \tag{1b}$$

This model is a generalization of the spherical shell model for which $\omega_1=\omega_2=\omega_3=\omega_0$ ($\beta=0$). In the original formulation of the model by Nilsson, and even in many subsequent applications, it is assumed that the nucleus is axially symmetric ($\omega_1=\omega_2=\omega\neq\omega_3$; $\beta\neq0$, $\gamma=0^\circ$). We have emphasized for many years the importance of nonaxial shapes ($\omega_1\neq\omega_2\neq\omega_3$; $\beta\neq0$, $\gamma\neq0$) in a dynamic theory of nuclear spectra.[6,17] Instead of assuming *a priori* whether a nucleus is spherical or deformed, axial or nonaxial, we let the collective Schrödinger equation govern the shape of the nucleus. The most

probable shape of a nucleus is not fixed in general but varies from one nuclear state to another.[18]

We also differ from the Nilsson model in (i) the method of relating the frequencies ω_k to nuclear shape variables (β, γ), and in (ii) the method of determining the model parameters.

Because of the short range of nuclear forces, the equipotential surfaces are expected to have the same shape as the nucleus. Hence, the vibrational frequency ω_k is assumed[8] to be inversely proportional to the semiaxis length R_k,

$$\omega_k = \omega_0 R_0/R_k \quad (k=1, 2, 3). \tag{2}$$

In the Nilsson model, the semiaxis lengths R_k of the nuclear ellipsoid are deduced from the Bohr-Mottelson definition[5, 10]

$$R(\theta, \phi) = R_0 \left[1 + \sum_M \beta_M Y^*_{2M}(\theta, \phi) \right] . \tag{3}$$

As is well known, Eq. (3) obeys the volume conservation condition $(R_1 R_2 R_3 = R_0^3)$ only to first order in β. In order to satisfy the condition exactly, Nilsson chose R_0, ω_0 in such a way that they also become functions of deformation.

Following Hill and Wheeler,[9] we define the semiaxes of the nuclear ellipsoid as

$$R_k = R_0 \exp[\delta \cos(\gamma - \tfrac{2}{3}\pi k)] . \tag{4}$$

On combining Eqs. (2) and (4), we get

$$\omega_k = \omega_0 \exp[-\delta \cos(\gamma - \tfrac{2}{3}\pi k)] . \tag{5}$$

Both Eqs. (4) and (5) conserve nuclear volume to all orders of deformation with *constant* R_0, ω_0. Also, Eq. (4) reduces to the Bohr-Mottelson definition if we keep terms only to first order in deformation and if we have

$$\delta = \beta[5/(4\pi)]^{1/2} . \tag{6}$$

Although both definitions allow for exact volume conservation, the β-γ dependence of R_k and ω_k is not the same. At small deformations, there is no difference. But at large deformations, the two potentials can be quite different for the same (β, γ).

On substituting Eq. (5) into Eq. (1), writing x_k^2 in terms of the spherical harmonics, and rearranging the terms, we get

$$H_{av} = H_0 + U_\beta , \tag{7}$$

where

$$H_0 = -[\hbar^2/(2M)]\nabla^2 + \tfrac{1}{2}M\omega_0^2 r^2 + \hbar\omega_0[v_{ll}(\vec{l}^2 - \langle \vec{l}^2 \rangle_N) + v_{ls}\vec{l}\cdot\vec{s}], \tag{8}$$

$$U_\beta = M\omega_0^2(\beta_{00} r^2 - \beta_0^P Q_{20} - \beta_{2'}^P Q_{22'}) , \tag{9}$$

$$\beta_{00} = \tfrac{1}{6}[\exp(-2\delta_x) + 2\exp(\delta_x)\cosh\delta_y - 3], \tag{10}$$

$$\beta_0^P = \tfrac{1}{6}(16\pi/5)^{1/2}[\exp(\delta_x)\cosh\delta_y - \exp(-2\delta_x)], \tag{11}$$

$$\beta_{2'}^P = \tfrac{1}{6}(48\pi/5)^{1/2}\exp(\delta_x)\sinh\delta_y , \tag{12}$$

$$\delta_x = \delta\cos\gamma, \quad \delta_y = \sqrt{3}\,\delta\sin\gamma , \tag{13}$$

and

$$Q_{20} = r^2 Y_{20}, \quad Q_{22'} = (1/\sqrt{2})r^2(Y_{22} + Y_{2,-2}) . \tag{14}$$

In the limit of small deformations, the potential U_β of Eq. (9) reduces to the average potential due to quadrupole force[6] because as $\beta \to 0$ we get

$$\beta_{00} \to 0, \quad \beta_0^P \to \beta_0 = \beta\cos\gamma, \quad \beta_{2'}^P \to \beta_{2'} = \beta\sin\gamma. \tag{15}$$

The "monopole" term contribution to the deforming potential of Eq. (9) is proportional to β_{00} and to $\langle r^2 \rangle \sim (\mathfrak{N} + \frac{3}{2})$. Hence, this term shifts the upper shells above the major shell and the lower shells below it, i.e., the effects of the usual quadrupole force are reduced. This term plays an important role in removing the divergence at large deformations caused by the usual quadrupole force when it is allowed to act in a large configuration space.[19]

The β-γ dependence of the potential deformations β_{00}, β_0^P, and $\beta_{2'}^P$ are given in Figs. 1 and 2. Figure 1 gives the β dependence for $\gamma = 0°$ in which case $\beta_{2'}^P = 0$. Figure 2 gives the γ dependence for $\beta = 0.6$.

The second difference between the present model and the Nilsson model, as mentioned above, is in the method of determining the model parameters. In the Nilsson model, the parameters v_{ls} and v_{ll} (Note that $v_{ls} = 2\chi_{\text{Nil}}$, $v_{ll} = -\chi_{\text{Nil}}\mu_{\text{Nil}}$) are determined by fitting the properties of odd-A nuclei. Although the same

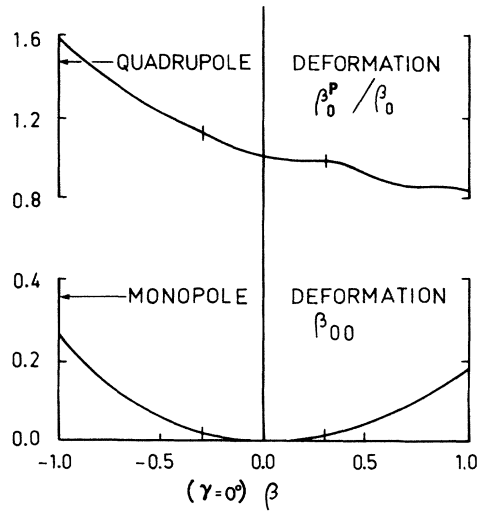

FIG. 1. β dependence of the monopole and quadrupole deformations of the modified Nilsson potential. The quantity β_0 equals β for the present case ($\gamma = 0°$), and $\beta_{2'}^P = \beta_{2'} = 0$. The vertical bars on the curves correspond to $|\beta| = 0.3$.

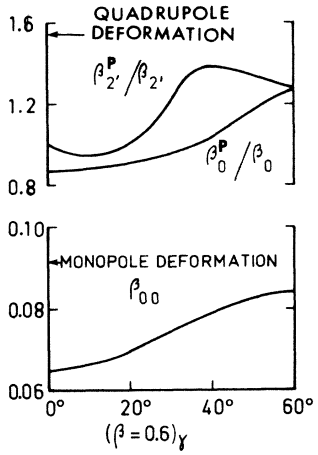

FIG. 2. γ dependence of the monopole and quadrupole deformations of the modified Nilsson potential. Definitions are given in the text.

values are used for all oscillator shells, the values depend on Z and A. Hence, it is necessary to generate the deformed-single-particle (DSP) basis for each nucleus.

We attempt to remove this complication by making the parameters v_{ll} and v_{ls} shell ($\mathfrak{N}$) dependent, instead of Z and A dependent. Furthermore, we assume that these parameters have the same values for neutrons and protons. These two unconventional assumptions are based on the following arguments.

(i) The odd-A spectra determine only a few levels near the Fermi surface (FS), i.e., only a few levels of the last major shell occupied by the nucleons. Hence, the empirical finding by Nilsson *et al.* that different v_{ll}, v_{ls} values are needed for different mass regions is taken into account in the present approach too.

(ii) Nilsson*et al.* employ different v_{ll}, v_{ls} values for neutrons and protons of the same nucleus. There is no strong experimental evidence for this. Spectra for odd-n and odd-p nuclei are quite similar in the case of light nuclei. True, such spectra are quite different in heavy nuclei. But this is taken into account in the present model partially by having different v_{ll}, v_{ls} values in different shells, and partially by employing an isospin-dependent oscillator energy constant [where the upper (lower) sign is for $\tau = p(n)$ for protons (neutrons)]

$$\hbar\omega_{0\tau} = (41\ \text{MeV})[1 \mp \tfrac{1}{3}(N-Z)/A]/A^{1/3} . \tag{16}$$

Note that the oscillator length constant also becomes isospin dependent since

$$b_\tau^{\,2} = \hbar/(M\omega_{0\tau}) . \tag{17}$$

The constant 41 MeV comes from the requirement that the nuclear radius is given approximately by[10]

$$R_0 = (1.2\ \text{fm})A^{1/3} . \tag{18}$$

The constant $\frac{1}{3}$ multiplying $(N-Z)/A$ in Eq. (16) comes from the requirement that neutrons and protons have approximately the same radii. Without this term neutrons in nuclei with substantial neutron excess would tend to have larger radii since $\langle r^2\rangle \sim (\mathfrak{N}+\frac{3}{2})b^2$ and N is larger for neutrons.[20]

(iii) By employing $\mathfrak{N}$-dependent v_{ll}, v_{ls}, we can make all the DSP basis wave functions and matrix elements independent of Z and A. In order to explain this point, let us recall a few steps used to solve the Hamiltonian defined by Eqs. (7)–(14). For simplicity, we drop the subscript τ. Define

$$\rho = r/b, \quad \rho_k = x_k/b . \tag{19}$$

Then, Eqs. (8) and (9) can be rewritten as

$$H_0 = \hbar\omega_0[-\tfrac{1}{2}\nabla_\rho^{\,2} + \tfrac{1}{2}\rho^2 + v_{ll}(\vec{l}^{\,2} - \langle\vec{l}^{\,2}\rangle_N) + v_{ls}\vec{l}\cdot\vec{s}] , \tag{20}$$

$$U_\beta = \hbar\omega_0(\beta_{00}\rho^2 - \beta_0^P Q'_{20} - \beta_{2'}^P Q'_{22'}) , \tag{21}$$

where

$$\nabla_\rho^2 = \sum_k \partial^2/\partial\rho_k^{\,2}, \quad Q'_{20} = Q_{20}/b^2$$

and

$$Q'_{22'} = Q_{22'}/b^2 . \tag{22}$$

Thus, the only Z-A dependence of our single-particle Hamiltonian is contained in the overall scaling factor $\hbar\omega_0$. The calculated wave functions $|p\rangle$ of the particle Schrödinger equation,

$$(H_0 + U_\beta)|p\rangle = \eta_p|p\rangle , \tag{23}$$

are independent of $\hbar\omega_0$. The eigenvalues η_p are simply proportional to $\hbar\omega_0$.

We solve the particle Schrödinger equation in a spherical basis, $|\mathfrak{N}lj\Omega m_t\rangle$, where Ω is the projection of $\vec{j}$ on the intrinsic Z axis, and $m_t = \frac{1}{2}$ $(-\frac{1}{2})$ for neutrons (protons). The $\Delta\mathfrak{N} = 2$, $\Delta j = 1$ and 2, and $\Delta\Omega = 2$ mixings caused by the deformed potential, U_β, are taken into account exactly in a large configuration space ($\mathfrak{N} = 0$–8). In our deformed single-particle basis, only parity $= (-1)^{\mathfrak{N}}$ and m_t remain as good quantum numbers. The degeneracy of time-reversal-conjugate orbits is maintained as usual. But because of $\Delta\Omega = 2$ mixing, it is not sufficient to consider only positive values of Ω. Instead, we choose

$$\Omega = \tfrac{1}{2}, -\tfrac{3}{2}, \tfrac{5}{2}, -\tfrac{7}{2}, \ldots \text{ for each } j . \tag{24}$$

As regards the $\mathfrak{N}$-dependent parameters v_{ll} and v_{ls}, their values are determined for low $\mathfrak{N}$ values ($\mathfrak{N} \leq 2$) in the usual way, i.e., by fitting the spectra of closed shell ± one nucleon nuclei. In the

case of higher $\mathfrak{N}$ values, we employ the stationarity conditions proposed recently by Yariv *et al.*[11]:

$$\frac{\partial(\delta U)}{\partial v_{ll}} = 0 = \frac{\partial(\delta U)}{\partial v_{ls}} , \tag{25}$$

where δU is the Strutinsky shell correction for a doubly magic nucleus. Actually, we employ a modified form of these conditions. Yariv *et al.* employed the same v_{ll}, v_{ls} values for all shells and obtained different sets of parameters for different nuclear regions.

We determine $\mathfrak{N}$-dependent ($\mathfrak{N}>2$) values of v_{ll}, v_{ls} by solving the stationarity conditions (25) *simultaneously* for all magic numbers (N or $Z=2$, 8, 20, 50, 82, 126, 184). Our parameters are given in Table I. Comparison with the calculations of Yariv *et al.* (when possible) shows that our parameters for the major shells just below the magic numbers are *identical*. But away from the FS our parameters are different.

Our spherical single-particle levels (valid for neutrons and protons in all nuclei, in the present model) are given in Table II. Note that our magic numbers are identical for neutrons and protons. The next proton magic number, $Z=126$, is in agreement with the early experiments[21] of Gentry *et al.* However, more recent experiments[21] by Sparks *et al.* cast serious doubt on earlier experiments. Hence, the question of next magic Z remains open.

The present single-particle basis is not large enough for well-deformed nuclei with $A>208$. But it can be used for heavier, spherical nuclei like those around the next magic number ($Z\simeq 126$).

Although hexadecapole (β_4) deformations are not introduced explicitly, the present basis contains some effects of such deformations (see Appendix I).

TABLE I. Parameters of the single-particle model.

$\mathfrak{N}$	$-v_{ls}$ [a]	$-v_{ll}$ [a]	Source
0	0.0	0.0	No effect on levels
1	0.204	0.0	Spectra [b] of ^{5}He, ^{5}Li, ^{15}N, ^{15}O
2	0.126	0.0	Spectra [b] of ^{17}O, ^{17}F, ^{39}K, ^{39}Ca
3	0.100	0.011	
4	0.184	0.037	Stationarity of Strutinsky Shell correction at magic numbers
5	0.140	0.026	
6	0.116	0.018	
7	0.086	0.014	
8	0.084	0.015	

[a] We follow the definitions of Bohr and Mottelson (see Ref. 10, Vol. 2), but differ from Nilsson (see Refs. 8 and 16) since $v_{ls}=-2\chi$, $v_{ll}=-\chi\mu$.

[b] See Ref. 10, Vol. 1.

TABLE II. Spherical-single-particle levels. Energies are given in units of $\hbar\omega_0$ which is slightly different for neutrons and protons if $Z\neq N$ (see text). Levels for the last shell are not complete since shells higher than $\mathfrak{N}=8$ are not included.

$\mathfrak{N}lj$	Energy	$\mathfrak{N}lj$	Energy
$0s_{1/2}$	1.500	126	
2		$6g_{9/2}$	7.394
		$6i_{11/2}$	7.636
$1p_{3/2}$	2.398	$6d_{5/2}$	7.762
$1p_{1/2}$	2.704	$7k_{15/2}$	7.905
8		$6g_{7/2}$	7.916
		$6s_{1/2}$	7.986
$2d_{5/2}$	3.374	$6d_{3/2}$	8.052
$2s_{1/2}$	3.500		
$2d_{3/2}$	3.689	184	
20		$7h_{11/2}$	8.355
		$7k_{13/2}$	8.550
$3f_{7/2}$	4.317	$7f_{7/2}$	8.693
$3p_{3/2}$	4.527	$8l_{17/2}$	8.744
$3f_{5/2}$	4.667	$7h_{9/2}$	8.828
$3p_{1/2}$	4.677	$7p_{3/2}$	8.919
$4g_{9/2}$	4.910	$7f_{5/2}$	8.994
50		$7p_{1/2}$	9.048
$4d_{5/2}$	5.612	258	
$4g_{7/2}$	5.738	$8i_{13/2}$	9.278
$5h_{11/2}$	5.890	$8l_{15/2}$	9.458
$4s_{1/2}$	6.018	$8g_{9/2}$	9.692
$4d_{3/2}$	6.072	$8i_{11/2}$	9.824
82		$8d_{5/2}$	9.986
		$8g_{7/2}$	10.070
$5f_{7/2}$	6.498	$8s_{1/2}$	10.160
$5h_{9/2}$	6.660	$8d_{3/2}$	10.196
$6i_{13/2}$	6.882		
$5p_{3/2}$	6.898		
$5f_{5/2}$	6.988		
$5p_{1/2}$	7.108		

III. DEFORMED-QUASIPARTICLE BASIS

The monopole pairing Hamiltonian is written as (we follow the notation of Kumar[22])

$$H_{\text{sta}} = H_{\text{av}} + U_P \tag{26a}$$

$$= \sum_p \eta_p C_p^\dagger C_p - \tfrac{1}{4} G \sum_{pq} S_p S_q C_{\bar{p}}^\dagger C_p^\dagger C_q C_{\bar{q}} , \tag{26b}$$

where H_{av} is the "average" one-body Hamiltonian described in Sec. II, η_p is an eigenvalue of H_{av}, G is the pairing force strength, S_p is a phase factor such that

$$S_p^2 = +1, \quad S_p S_{\bar{p}} = -1, \qquad S_p \xrightarrow{\beta\to 0} (-1)^{j_p - l_p + \Omega_p} \tag{27}$$

and $|\bar{p}\rangle$ denotes a time-reversed state of $|p\rangle$.

Since the DQP basis does not conserve the number of particles, one introduces a Lagrange mul-

tiplier λ and considers the solutions of the modified Hamiltonian

$$H'_{\rm sta} = H_{\rm sta} - \lambda \hat{N} , \tag{28a}$$

where $\hat{N}$ is the particle number operator,

$$\hat{N} = \sum_p C_p^\dagger C_p . \tag{28b}$$

Value of the Lagrange multiplier λ is determined by accepting only those solutions of $H'_{\rm sta}$ which satisfy the condition

$$\langle \hat{N} \rangle = N , \tag{29}$$

where N is the number of nucleons (neutrons or protons).

The major effects of the two-body pairing force of Eqs. (26) and (27) are usually taken into account via a transformation from the particle, hole operators $(C_p^\dagger, C_p)$ to quasiparticle operators

$$A_p^\dagger = U_p C_p^\dagger - V_p S_p C_{\bar{p}} , \tag{30a}$$

$$A_p = U_p C_p - V_p S_p C_{\bar{p}}^\dagger . \tag{30b}$$

The mixing amplitudes, or the U-V factors, are determined via the Bogolyubov conditions[23]

$$\langle pq | H'_{\rm sta} | 0 \rangle = 0 \text{ for all } p,q \tag{31}$$

and

$$\langle p | H'_{\rm sta} | q \rangle = E_p \delta_{pq} . \tag{32}$$

The quasiparticle states $|0\rangle$, $|p\rangle, \ldots$ are defined via the equations

$$A_p |0\rangle = 0 \quad \text{for all } p, \tag{33a}$$

$$|p\rangle = A_p^\dagger |0\rangle , \tag{33b}$$

$$|pq\rangle = A_p^\dagger A_q^\dagger |0\rangle . \tag{33c}$$

These conditions lead to the BCS pairing equations,

$$2V_p^2 = 1 - (\eta_p - \lambda)/E_p , \tag{34}$$

$$U_p^2 = 1 - V_p^2 , \tag{35}$$

$$E_p^2 = (\eta_p - \lambda)^2 + \Delta^2 , \tag{36}$$

$$2G^{-1} = \sum_p{}' E_p^{-1} , \tag{37}$$

and

$$N = \sum_p{}' 2V_p^2 , \tag{38}$$

where Δ is the energy gap parameter [values of Δ and λ are determined by solving Eqs. (37) and (38)], and $\sum'$ denotes summation over direct states only [see Eq. (24) for our definition of such states].

The BCS equations allow us to include the major effects of two-body pairing correlations in a redefined single-particle basis, called quasiparticle (spherical only) or deformed-quasiparticle (deformed as well as spherical) basis. But it has been known for a long time that many higher order terms are neglected. There exists a large body of literature dealing with one or more of these terms—for instance, improvement of the treatment of particle number conservation. Most of the proposed treatments make the treatment of pairing so complicated that many other important effects (for instance, the dynamics of nuclear deformations) have to be neglected. We discuss below a simple modification which allows us to include some higher order terms.

Using the general relations[22] for the matrix elements of one-body and two-body operators in a DQP basis, we find that the Bogolyubov conditions (31) and (32) lead to

$$2U_p V_p (\eta_p - \lambda - GV_p^2) - G(U_p^2 - V_p^2) \sum_c{}' U_c V_c = 0 , \tag{39}$$

$$(U_p^2 - V_p^2)(\eta_p - \lambda - GV_p^2) + 2GU_p V_p \sum_c{}' U_c V_c = E_p . \tag{40}$$

In the BCS theory, the GV_p^2 terms of Eqs. (39)–(40) are neglected. These terms come from the particle-hole type of matrix elements of the pairing force, $\langle p\bar{c} | U_P | q\bar{c} \rangle$, while the terms proportional to $G\sum_c' U_c V_c$ come from the particle-particle (or hole-hole) matrix elements, $\langle p\bar{q} | U_P | \bar{c}c \rangle$ [see Eqs. (69)–(72) of Ref. 22]. The GV_p^2 term produces a kind of Blocking effect since the occupied levels are pushed down. On solving Eqs. (39) and (40) in the usual way, we find that Eqs. (35), (37), and (38) remain valid but Eqs. (34) and (36) become (for $\Delta \neq 0$)

$$2V_p^2 = 1 - (\eta_p - \lambda - \tfrac{1}{2}G)/(E_p - \tfrac{1}{2}G) \tag{34'}$$

$$E_p = \tfrac{1}{2}G + (E_p/\Delta)[(E_p - \tfrac{1}{2}G)^2 - (\eta_p - \lambda - \tfrac{1}{2}G)^2]^{1/2} . \tag{36'}$$

In the case of $\Delta = 0$ [when G is too small to satisfy Eq. (37) for $\Delta \neq 0$], we examine the equations carefully and find the following solutions,

$$U_p = 0, \quad V_p = 1, \quad E_p = \tfrac{1}{2}G + (\lambda + \tfrac{1}{2}G - \eta_p) \quad \text{if } \eta_p < (\lambda + \tfrac{1}{2}G) , \tag{41a}$$

$$U_p = 1/\sqrt{2}, \quad V_p = 1/\sqrt{2}, \quad E_p = \tfrac{1}{2}G \quad \text{if } \eta_p = (\lambda + \tfrac{1}{2}G) , \tag{41b}$$

$$U_p = 1, \quad V_p = 0, \quad E_p = \tfrac{1}{2}G + (\eta_p - \lambda - \tfrac{1}{2}G) \quad \text{if } \eta_p > (\lambda + \tfrac{1}{2}G) . \tag{41c}$$

Note that while in the BCS theory, the quasiparticle energy E_p vanishes if $\Delta = 0$ and $\eta_p = \lambda$ [see Eq. (36)], this energy never vanishes in the present theory. Its minimum value is given by $\frac{1}{2}G$—a

positive, nonzero number. This helps us to remove a long standing problem which occurred when two levels crossed near the Fermi energy (λ in the BCS theory) and Δ was vanishingly small. Then the energy denominator entering the expressions for the moments of inertia (see Sec. V) would be vanishingly small ($E_p + E_q \to 0$). In the present theory, this energy denominator (energy of a two-quasiparticle state above the zero-quasiparticle state) is given by

$$E_{pq} = \langle pq | H_{\text{sta}} | pq \rangle - \langle 0 | H_{\text{sta}} | 0 \rangle \tag{42a}$$

$$E_{pq} = E_p + E_q - G\Delta^2/(2E_p E_q), \quad q \neq \bar{p}\ , \tag{42b}$$

$$E_{p\bar{p}} = 2E_p - G. \tag{42c}$$

Of course, $q = p$ is forbidden by the Pauli principle. For $q \neq \bar{p}$, this energy denominator goes in the limit of $\Delta \to 0$, $\eta_p \to \lambda + \frac{1}{2}G$, $\eta_q \to \lambda + \frac{1}{2}G$ to the value of G. It does not vanish. The problem does not arise in the case of $q = \bar{p}$ (see Sec. V). Thus, the divergence coming from this type of situation in the BCS theory is removed in our improved theory.

As regards an increase in the complexity of computations, this increase is very slight. The main difference from the earlier equations is in our Eq. (36′) for the quasiparticle energy. This is an iterative equation. But a good initial guess to the initial value of E_p is provided by the BCS Eq. (36). When this value is substituted in Eq. (36′), one iteration leads to a good convergence in the case of most single-particle levels. The levels nearest the Fermi surface require the largest number of iterations. In the many cases, where we studied this question, the maximum number of needed iterations was 3–5.

As regards the pairing force constant, we employ the parametrization

$$G_{p,n} = G_0[1 \pm G_1(N - Z)/A]\ . \tag{43}$$

The constants G_0, G_1 (or G_p, G_n) are often determined by fitting the odd-even mass differences. But we prefer to employ different methods for G_0 and G_1.

The observed nuclear property most sensitive to the value of G_1 is the gyromagnetic ratio (or half the magnetic moment of the first 2 + state of a well-deformed nucleus). This ratio is remarkably constant for well-deformed nuclei with $A = 150$–186 and is ~ 0.3 within a few percent.[24] We employ this fact to fix the parameter

$$G_1 = 0.3. \tag{44}$$

Following Bohr and Mottelson,[10] we determine the value of G_0 (the average of proton and neutron values) by fitting the extra binding energy of nuclei with two nucleons outside (or holes inside) a closed shell. This problem is solved *exactly* by considering two nucleons interacting via the pairing force of Eqs. (26a) and (26b). The dispersion equation to be solved is

$$G^{-1} = \sum_p{}' (2|\eta_p - \eta_0| - E)^{-1}\ , \tag{45}$$

where η_0 is the energy of the single-particle level occupied by the last two nucleons. The dispersion Eq. (45) may be solved, for a given G value, to determine the various eigenvalues E. But we are interested in determining the G value for a specific E value (the lowering of the ground state due to pairing correlations) which is deduced from the experimental masses (separation energies) via the relations for neutron pairing,

$$E(Z,\ N-2) = -[2S_n(Z, N) - S_{2n}(Z, N)], \tag{46a}$$

$$E(Z, N+2) = -[S_{2n}(Z, N+2) - 2S_n(Z, N+1)], \tag{46b}$$

where Z and N are *both* magic numbers. Similar relations hold for protons.

Using Eqs. (45)–(46) for 12 nuclei around magic numbers (8, 8), (20, 20), and (82, 126), we obtain 12 pairing force constants whose average value is (see Fig. 3)

$$G_0 = 17\ \text{MeV}/A\ . \tag{47}$$

Figure 3 also depicts the convergence of G with the number of single-particle levels included in the summation in Eq. (45). An equal number of

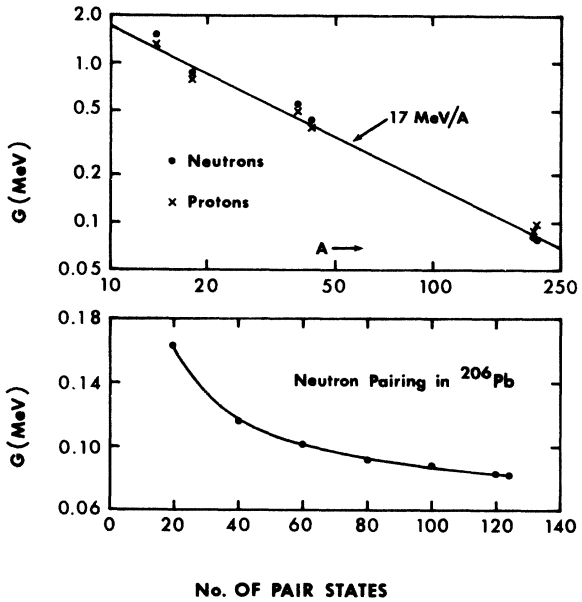

FIG. 3. Pairing force strength deduced from the pair binding energies. The lower part of the figure depicts the convergence with the number of pair states included in the calculation. The upper part of the figure (a log-log plot) is employed to determine the A dependence as well as the strength of the pairing force.

levels below and above the Fermi energy are included in each case. In the final calculations, all levels below ($N/2$ or $Z/2$) and an equal number above are included.

The two pairing constants of Eqs. (44) and (47) are used in all the calculations reported in the rest of this paper.

IV. POTENTIAL ENERGY OF DEFORMATION

A general Hamiltonian for the unified treatment of intrinsic motion (motion of individual nucleons with respect to intrinsic axes attached to the nucleus) and collective motion (rotation and vibration of the nucleus as a whole) may be written as

$$H = H_{\rm sta}\left(\vec{\mathbf{x}}, \alpha_\mu, \frac{\partial}{\partial \vec{\mathbf{x}}}\right) + H_{\rm dyn}\left(\vec{\mathbf{x}}, \alpha_\mu, \frac{\partial}{\partial \alpha_\mu}, \frac{\partial}{\partial \vec{\mathbf{x}}}\right), \quad (48)$$

where $\vec{\mathbf{x}}$ represents the intrinsic coordinates and α_μ the collective variables. In general, the two types of motion cannot be separated from each other. But, the many successes of the rotational model[10] suggest that the coupling term is negligible for the low energy states of even-even nuclei. Then, we can employ the Born-Oppenheimer approximation.[25] In this approximation, the problem is divided into two steps (see Ref. 14 for a beautiful discussion.)

First, we keep the collective variables α_μ fixed (e.g., the distance between the two atoms of a diatomic molecule) and solve the eigenvalue problem

$$H_{\rm sta}\left(\vec{\mathbf{x}}, \alpha_\mu, \frac{\partial}{\partial \vec{\mathbf{x}}}\right) X(\vec{\mathbf{x}}, \alpha_\mu) = V(\alpha_\mu) X(\vec{\mathbf{x}}, \alpha_\mu) \quad (49)$$

for each set α_μ. The eigenvalues of this "intrinsic" equation, which are functions of α_μ, form the potential energies of the second step where we solve the equation

$$H\Psi(\vec{\mathbf{x}}, \alpha_\mu) = E\Psi(\vec{\mathbf{x}}, \alpha_\mu) \quad (50a)$$

in the basis

$$\Psi(\vec{\mathbf{x}}, \alpha_\mu) = X(\vec{\mathbf{x}}, \alpha_\mu)\psi(\alpha_\mu)\,. \quad (50b)$$

On multiplying both sides of Eq. (50a) by $X^*(\vec{\mathbf{x}}, \alpha_\mu)$ and integrating over $\vec{\mathbf{x}}$, we get a purely collective Schrödinger equation (CSE)

$$\left[T_{\rm coll}\left(\alpha_\mu, \frac{\partial}{\partial \alpha_\mu}\right) + V(\alpha_\mu)\right]\psi(\alpha_\mu) = E\psi(\alpha_\mu). \quad (51)$$

We approximate $H_{\rm sta}$ of Eqs. (48) and (49) by the pairing Hamiltonian of Eqs. (26a) and (26b) which included deformations via the average part $H_{\rm av}$. Then, solutions of the eigenvalue equation (49) are given by

$$X(\vec{\mathbf{x}}, \alpha_\mu) \equiv |n\rangle, \quad (52)$$

where $n = 0, 2, 4, \ldots$ for even-even nuclei; $1, 3, 5, \ldots$ for odd-A nuclei; $2, 4, 6, \ldots$ for odd-odd nuclei. States with $n = 0, 1, 2$ are defined by Eq. (33). Those with larger number of quasiparticles can be constructed in a similar manner. We can have collective states built on top of each of these states (or, a linear combination of them).

In this paper, we consider two types of tests of this basis of states. Both of them refer to the low-energy states of even-even nuclei. For this purpose, we consider only the $n = 0$ state. Then, the eigenvalue of Eq. (49) is given by

$$V_0 = \langle 0 | H_{\rm sta} | 0\rangle = \langle 0 | H'_{\rm sta} + \lambda \hat{N} | 0\rangle, \quad (53)$$

where we have used Eq. (28a). Using the general relations[22] for the matrix elements of one-body and two-body operators, we obtain

$$V_0 = \sum_\tau \left(\sum_q{}' 2V_q{}^2 \eta_q - \Delta^2/G - G\sum_q{}' V_q{}^4\right)_\tau, \quad (54)$$

where $\tau = p$, n for protons, neutrons (as usual, the pairing calculation is done separately for protons and neutrons).

It is now generally[1-4] recognized that the potential energy of Eq. (54) needs to be corrected via the Strutinsky shell correction method. The argument may be stated as follows. The experimental spectra of odd-A nuclei determine at best only a few single-particle levels near the Fermi surface. Hence, we cannot expect the energy of Eq. (54) to give correctly the long range behavior—the contributions of levels far from the FS. In the Strutinsky method, it is assumed that the long range behavior is given correctly by the liquid drop model whose parameters are determined by fitting all known nuclear masses. The short range behavior is attributed to the bunching of the single-particle levels (instead of being uniformly distributed). Thus, the corrected potential energy is written as

$$V = V_{\rm LDM} + \delta U + \delta V_P, \quad (55)$$

where $V_{\rm LDM}$ is the deformation energy of the LDM nucleus, δU is the shell correction given by

$$\delta U = \sum_\tau \left[2\sum_{\eta<\lambda}{}' \eta_q - 2\int_{-\infty}^{\bar\lambda} \eta \bar\rho(\eta) d\eta\right]_\tau, \quad (56)$$

δV_P is the pairing correction given by

$$\delta V_P = V_0 - V_0(\Delta = 0) \quad (57a)$$

$$= V_0 - \sum_\tau \left(2\sum_{\eta<\lambda}{}' \eta_q - \tfrac{1}{2}GN\right)_\tau, \quad (57b)$$

$\bar\rho(\eta)$ is the level density (obtained after spreading each level over a width of Γ), and $\bar\lambda$ is the Fermi energy obtained by solving the particle number equation

$$N = 2\int_{-\infty}^{\bar\lambda} \bar\rho(\eta) d\eta\,. \quad (58)$$

We calculate the shell correction up to sixth or-

der[2] in $(\eta-\eta_q)/\Gamma$. The value of the width parameter Γ is determined for each nucleus via the stationarity condition

$$\frac{\partial}{\partial\Gamma}(\delta U_S)=0 \text{ (spherical case)}, \tag{59a}$$

$$\frac{\partial}{\partial\Gamma}(\delta U_S-\delta U_D)=0 \text{ (deformed case)}. \tag{59b}$$

This condition depends somewhat on the deformation of the nucleus. We choose that deformation which minimizes the total potential energy V. Two examples are given in Fig. 4.

In order to calculate $V_{\rm LDM}$ we chose the recent parametrization of Seeger and Howard.[26] The deformation-dependent part of their expression for the LDM energy is given by

$$V_{\rm LDM}=\frac{\beta(N-Z)^2}{A}\left(\frac{1}{1+3.28B_sA^{-1/3}}-\frac{1}{1+3.28A^{-1/3}}\right)+\gamma A^{2/3}(B_s-1)-\phi A^{1/3}(B_k-1)$$

$$+\tfrac{3}{5}Z(Z-1)(e^2/R)[1+18.0295(a/R)^3-85.2330(a/R)^4](B_C-1),$$

$$\beta=33.166 \text{ MeV}, \quad \gamma=17.073 \text{ MeV}, \quad \phi=-0.76 \text{ MeV}, \quad a=0.513 \text{ fm}, \quad R=1.2254A^{1/3} \text{ fm}. \tag{60}$$

The functions B_s, B_C, and B_k are the surface, Coulomb, and curvature shape dependences of the liquid drop, normalized to unity for spherical shapes. These functions are usually computed for axially symmetric shapes, see for example the tables given by Seeger and Howard.[26] But in our dynamic theory of deformations, we need to consider nonaxial shapes ($\gamma\neq 0°$). Also, we employ a somewhat unusual definition of deformations, the Hill-Wheeler definition of Eq. (4). Therefore, we give our method of calculating these functions in Appendix II.

Our calculated potential energy functions of deformation are given for three sets of transitional nuclei in Figs. 5–7. The full γ dependence is employed for the dynamic calculations. Also, the equilibrium shape of a transitional nucleus is quite sensitive to the β-γ dependence of the inertial functions. Still, the axial ($\gamma=0°$) plot of the potential function $V(\beta,\gamma)$ provides a first clue to some basic properties of a nucleus — whether spherical or deformed, prolate or oblate, rigid or soft against vibrations.

One of the traditional tests of such calculations is based on the spherical-deformed shape transi-

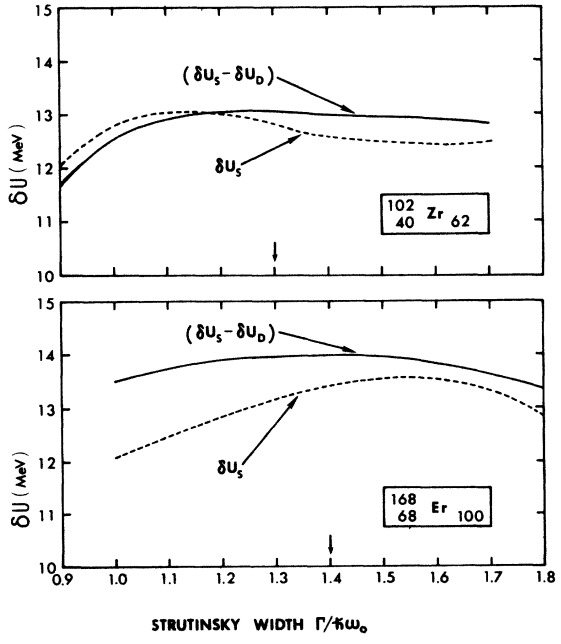

FIG. 4. Variation of Strutinsky shell correction with the Strutinsky width parameter. The quantities $\delta U_S, \delta U_D$ represent shell corrections for spherical, deformed (potential minimum) shapes.

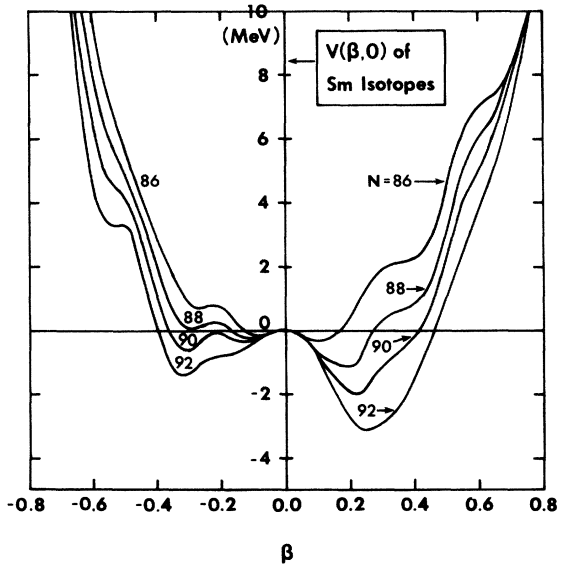

FIG. 5. $V(\beta,0)$ of Sm isotopes. The potential energy is normalized to zero for the spherical shape. The "minima" on the oblate side ($\beta<0$) are not true minima but saddle points (maxima in γ direction). The prolate "minima" for $N=86$, 88 are unstable against zero-point motion.

tion in Sm isotopes as the neutron number changes from $N=88$ to $N=90$. Our DQP basis passes this test, see Fig. 5 for plots of $V(\beta, 0)$ for $^{148, 150, 152, 154}_{62}$Sm. True, we get nonspherical potential minima for $^{148, 150}$Sm. But such shallow minima are easily washed out by the zero-point energy. In our previous, dynamic[12] calculation for ^{150}Sm, the potential minimum was 1.2 MeV below the spherical energy. Still, the zero-point energy of 0.9 MeV led to a spherical maximum in the ground state wave function.

Another important test of such calculations is provided by the prolate-oblate shape transition in the Os isotopes at $N \sim 116$. This transition is more gradual compared with the $N=88-90$ transition, since the change in γ_{min} is accompanied by a reduction in β_{min} as N approaches the magic number 126. But, the plots of $V(\beta, 0)$ of $^{186, 188, 190, 192, 194}_{76}$Os given in Fig. 6 show the expected trends and agree with our previous calculations[7] (which were the first calculations to provide detailed explanations for the properties of these nuclei, see the discussion of these results in Refs. 14 and 44).

During recent years, there has been much interest in the Hg isotopes. Bonn *et al.*[27] have deduced from their optical pumping experiments that the nuclear radius shows an unusually large increase between $A=185-187$. Foucher *et al.*[28] have studied the systematics of a large number of properties in this region and proposed that Hg nuclei of unstable oblate shape become critical nuclei (unstable against β vibrations, γ vibrations, pairing fluctuations, and octupole vibrations) at $A=186$. Hamilton *et al.*[29] have discovered the coexistence of near spherical and deformed bands in $^{186, 188}$Hg. More recently, Cole *et al.*[30] have found an excited deformed band in ^{184}Hg with its $0'^{+}$ state only 8 keV above the first 2^{+} state. All these studies show that something unusual happens around ^{186}Hg.

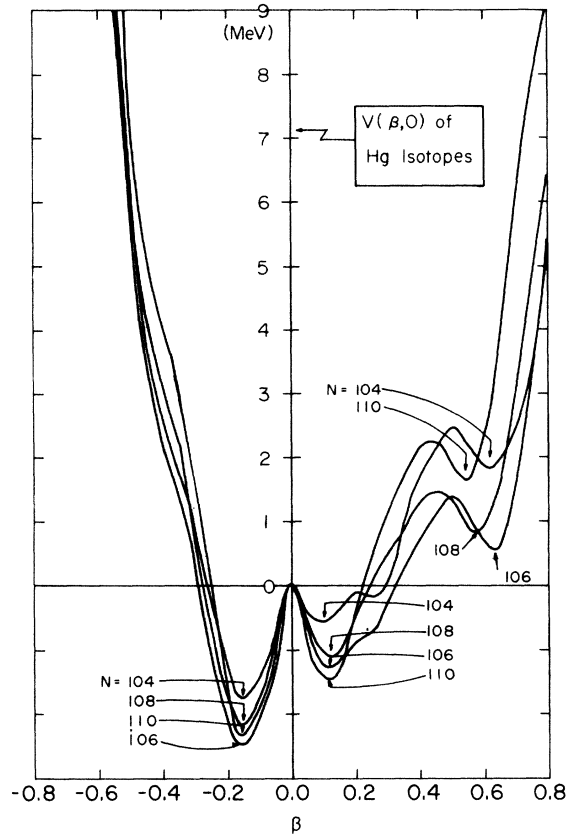

FIG. 7. $V(\beta, 0)$ of Hg isotopes. Note that the nucleus does not get more and more deformed as we go away from the closed shell at $N=126$. Instead, the lowest minimum occurs for $^{186}_{106}$Hg.

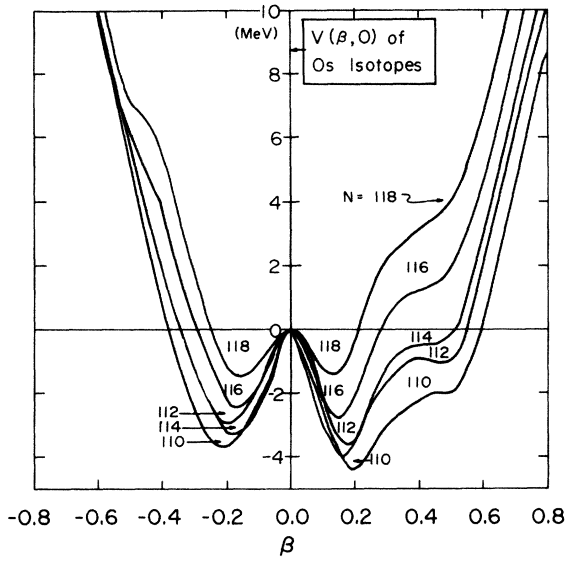

FIG. 6. $V(\beta, 0)$ of Os isotopes. Note that the prolate oblate difference, $V_{po}=V(-|\beta_{min}|, 0)-V(|\beta_{min}|, 0)$, decreases from 0.8 MeV for $^{186}_{110}$Os to -0.1 MeV for $^{194}_{118}$Os.

Our potential plots for $^{184, 186, 188, 190}_{80}$Hg, see Fig. 7, agree qualitatively with some of the above expectations. Normally, we expect the nuclei to get more deformed as we go away from closed shells. Instead, we find that as we go from ^{190}Hg to ^{184}Hg ($N=110-104$), the potential minimum gets shallower (110–108), deeper (108–106), and shallower again (106–104). Among these four isotopes, the deepest minimum occurs for ^{186}Hg. This peculiar behavior is related to the fact that protons of these nuclei are only two nucleons away from the closed shell at $Z=82$. Hence, the calculated proton energy gap vanishes at equilibrium shapes (lowest potential minima). This fact is also responsible for the

appearance of a second minimum at large, prolate deformations ($\beta \approx 0.6$). Note that the "minimum" at $\beta \approx 0.1$ is not a true minimum but a saddle point (minimum along β but maximum along γ).

For a detailed explanation of the properties of Hg and other nuclei, we need to consider the dynamics and calculate the spectra. This is the subject of the next section, where it is pointed out (also, in the introduction) that the present version of the dynamic theory is not valid for soft, transitional nuclei.

V. DYNAMICS OF DEFORMATION

A microscopic method of solving the dynamics of nuclear deformations has been proposed and applied by Kumar and Baranger.[6, 7, 12] This method has been quite successful for the transitional nuclei of the osmium region,[7] and of the samarium region.[12] Recently, it has been extended to well-deformed nuclei in the gadolinium region.[48] But this method has also come under some criticism.

The Kumar-Baranger method was based on the pairing-plus-quadrupole model of nuclear interactions. This model seemed to be closer to first principles since the nuclear deformations arise as a consequence of a two-body, quadrupole force rather than assumed to exist in the average field as in the Nilsson model. But a severe problem with the quadrupole force, as pointed out previously,[19] is that this force is reasonable only in a truncated configuration space.

Hence, the configuration space employed in these calculations had to be limited to two oscillator shells near the FS. Thus, in addition to the strength of the quadrupole force, it was necessary to use two more parameters—an additive[7] or multiplicative[12, 48] parameter for the inertial functions (moments of inertia and mass parameters), and an effective charge for $E2$ moments. Also, different sets of spherical, single-particle levels had to be employed for the $A \sim 190$ (Ref. 7) and $A \sim 150$ (Refs. 12 and 48) regions. This has been a major hindrance in extending the model to different nuclear regions.

During the past eight years, we have investigated several methods of improving the radial dependence of the quadrupole force—with the idea of extending the configuration space and reducing the number of parameters. One of these methods was based on a radial dependence[31] derived from a Woods-Saxon potential. Others[32] were based on modifications of the radial matrix elements of the quadrupole force so that they do not increase with the oscillator shell number ($\mathfrak{N}$) and/or they do not cause too much mixing of type $\Delta\mathfrak{N} = 2$. All these methods were found to be unsatisfactory.

Better mathematical treatments of the pairing-plus-quadrupole model have recently been made by Kishimoto and Tamura,[49] who employ boson expansion methods, and by Faessler *et al.*,[50] who employ projection methods. However, both groups employ configuration spaces which are much smaller than ours (Sec. II).

Another recent development in this respect has been in the Hartree-Fock treatment of realistic and semirealistic forces. Impressive gains have been made by several groups, see the review papers by Vautherin[33] and Gogny.[34] However, in these methods, just the calculation of the axial part of the potential energy surface is so time-consuming that the calculation of the full dynamics (inclusion of the γ degree of freedom and the calculation of the inertial functions) appears to be prohibitive at least at the present time.

Hence, we come back to the point of view based on the Nilsson model which predates both the quadrupole force model as well as the Hartree-Fock theory of deformations. One can argue that a deformed-single-particle model is just as fundamental or empirical as the spherical-single-particle model. If we drop the assumption that the oscillator frequencies are equal in all directions ($\omega_1 = \omega_2 = \omega_3$), then we get a more general model which includes the spherical model as a special case. Also, most nuclei are closer to a polyatomic molecule (a system with several centers of force, hence the average field is nonspherical) rather than an atom (a system with a single center of force generating a spherically symmetric field).

As regards the method of determining the collective kinetic energy, two methods exist. In the cranking model method,[35-37] one adds a time-dependent field ($H_{\rm dyn} = i\hbar\dot{\alpha}_\mu \partial/\partial\alpha_\mu$) to the static field represented by $H_{\rm sta}$. In the time-dependent Hartree-Bogolyubov method,[38, 45] no additional term is added to the microscopic Hamiltonian. But time-dependent terms are added to the wave function, the argument being that the static Hartree-Fock gives only the instantaneous (fixed α_μ) wave function. Both methods use perturbation theory up to second order in $\dot{\alpha}$ and lead to the same expression for the collective kinetic energy

$$T_{\rm coll} = \frac{1}{2}\sum_{\mu\nu} B_{\mu\nu}\dot{\alpha}_\mu\dot{\alpha}_\nu^* , \tag{61}$$

$$B_{\mu\nu} = \sum_{p\,q} E_{pq}^{-3}\,(C_\mu)_{pq}\,(C_\nu)_{pq}^* , \tag{62a}$$

$$(C_\mu)_{pq} = (U_p V_q + V_p U_q)\langle p|\partial H_{\rm av}/\partial\alpha_\mu|q\rangle + \delta_{pq}[(U_p^2 - V_p^2)\partial\Delta/\partial\alpha_\mu + 2U_p V_p\,\partial\lambda/\partial\alpha_\mu], \tag{62b}$$

where E_{pq} is the energy of a two-quasiparticle

state $|pq\rangle$ measured from the zero-quasiparticle state $|0\rangle$. Note that in the BCS theory, the energy E_{pq} equals $E_p + E_q$, while in our improved pairing theory it is given by Eq. (42). The relations (61) and (62) are valid for any collective variables α_μ. But in the following discussions, we restrict ourselves to the quadrupole variables

$$\alpha_\mu = \beta_\mu \equiv \beta_{2\mu} \quad (\mu = 0, \pm 1, \pm 2), \tag{63a}$$

$$|\beta_\mu|^2 = \beta^2 , \tag{63b}$$

where β is the deformation variable defined by Eqs. (4) and (6).

In the quadrupole force model,[38] the operator $\partial H_{\rm av}/\partial\beta_\mu$ is given by

$$\partial H_{\rm av}/\partial\beta_\mu = -\hbar\omega_0 Q'^{*}_{2\mu} . \tag{64}$$

It is simply proportional to the quadrupole operator. However, it takes a more complicated form for the modified Nilsson model discussed in Sec. II. In order to give the equivalent form for Eq. (64), we would first need to transform the Hamiltonian of Eqs. (7), (20), and (21) to the lab system. However, the actual calculations are done in the intrinsic representation. So, for the sake of brevity, we will not write down the equivalent form of Eq. (64).

As mentioned above, the actual computations are performed in the intrinsic representation (two shape variables β and γ; three Euler's angles ϕ, θ, and ψ) where the collective kinetic energy is written as[38,39]

$$T_{\rm coll} = T_{\rm rot} + T_{\rm vib} , \tag{65a}$$

$$T_{\rm rot} = \frac{1}{2}\sum_{k=1}^{3} \mathcal{I}_k(\beta_0, \beta_2')\omega_k^2 , \tag{65b}$$

$$T_{\rm vib} = \frac{1}{2}\sum_{ab} B_{ab}(\beta_0, \beta_2')\dot\beta_a\dot\beta_b , \tag{65c}$$

where a or $b = 0, 2'$; ω_k are the rotational frequencies [certain linear combinations of $\dot\phi$, $\dot\theta$, and $\dot\psi$ which allow us to write $T_{\rm rot}$ in the form of Eq. (65b)]; β_0, β_2' are defined by Eq. (15). The moment of inertia functions are given by the "cranking model" type of expression

$$\mathcal{I}_k(\beta_0, \beta_2') = 2\sum_{p<q}{}' E_{pq}^{-1}(U_p V_q - V_p U_q)^2 |\langle p|J_k|q\rangle|^2 , \tag{66}$$

where J_k is the kth component of the *nucleon* angular momentum operator. The mass parameter functions are given by

$$B_{ab}(\beta_0, \beta_2') = 2\left[\sum_{p<q}{}' E_{pq}^{-3}(U_p V_q + V_p U_q)^2 \left\langle p\left|\frac{\partial H_{\rm av}}{\partial\beta_a}\right|q\right\rangle\left\langle q\left|\frac{\partial H_{\rm av}}{\partial\beta_b}\right|p\right\rangle + \sum_{p}{}' E_{p\bar p}^{-3} C_{ap} C_{bp}\right] , \tag{67}$$

$$C_{ap} = 2U_p V_p\left(\left\langle p\left|\frac{\partial H_{\rm av}}{\partial\beta_a}\right|p\right\rangle + \frac{\partial\lambda}{\partial\beta_a}\right) + (U_p^2 - V_p^2)\frac{\partial\Delta}{\partial\beta_a} . \tag{68}$$

The derivatives $\partial\lambda/\partial\beta_a$, $\partial\Delta/\partial\beta_a$ are determined analytically by using Eqs. (125a)–(126d) of Ref. 38, where the operator Q_μ is replaced by $\partial H_{\rm av}/\partial\beta_\mu$. Using Eqs. (6)–(14), (20), and (21) for the definition of $H_{\rm av}$, we get

$$\partial H_{\rm av}/\partial\beta_a = \hbar\omega_0(D_a\rho^2 + E_a Q'_{20} + F_a Q'_{22'}), \tag{69a}$$

where

$$D_a = \frac{5}{4\pi}\beta_a^P, \quad E_0 = 2\beta_{00} + 1 - \beta_0^P\left(\frac{5}{4\pi}\right)^{1/2}, \tag{69b}$$

$$E_{2'} = F_0 = \beta_{2'}^P\left(\frac{5}{4\pi}\right)^{1/2}, \quad F_{2'} = 2\beta_{00} + 1 + \beta_0^P\left(\frac{5}{4\pi}\right)^{1/2} . \tag{69c}$$

Note that the $C_{ap}C_{bp}$ term of the mass parameters of Eq. (67) is a purely pairing term. It represents the effects of pairing fluctuations. This term vanishes in the limit $\Delta \to 0$. Hence, the calculation is not affected by the possible vanishing of $E_{p\bar p}$ [see Eqs. (42c) and (41b)] in this limit. The other energy denominators appearing in our expressions for the mass parameters (67) and the moments of inertia (66) depend on E_{pq} ($q \neq p$ or $\bar p$), which never vanishes in our version of the pairing theory (see Sec. III).

After calculating the inertial functions and the potential function of deformation, the next step consists of solving the collective Schrödinger equation (51). This is done in the numerical solution method of Kumar and Baranger,[39] later modified by Kumar.[12,40] Some preliminary results for ^{168}Er, ^{102}Zr, and ^{24}Mg are given in Tables III–V and Figs. 8–12.

In the present method of calculation, we do not assume the nucleus to be vibrational or rotational. Instead, we solve numerically a Hamiltonian for each value of nuclear angular momentum ($I = 0, 2, 3, 4, 5, 6$; parity = positive for all states). However, for the sake of discussion of the results, we group the calculated states into rotational bands built on different intrinsic or vibrational states. For this purpose, we look at the calculated wave functions of each state—especially at the largest K compon-

TABLE III. Energy levels and wave functions for $^{102}_{40}Zr_{62}$.

Most prob. K	I	Excitation energy (MeV) Ex.[a]	Th.	Wave function max. at β	γ (deg)	Calc. wave functions % K Component $K=0$	$K=2$	$K=4$	$K=6$
0	0	0.0	0.0	0.409	12	100.0			
	2	0.152	0.132	0.409	12	99.8	0.2		
	4	0.479	0.469	0.409	12	99.5	0.4	0.1	
	6	0.965	1.008	0.409	12	98.5	1.2	0.2	0.0
2	2		0.823	0.391	34	7.9	92.1		
	3		1.281	0.397	19	0.0	100.0		
	4		1.319	0.391	34	20.3	75.5	4.2	
	5		1.858	0.397	19	0.0	97.7	2.3	
	6		1.960	0.397	19	22.6	69.2	7.3	1.0
0	0		0.840	0.350	38	100.0			
	2		1.207	0.391	34	90.3	9.7		
	4		1.773	0.391	34	44.1	33.3	22.6	
	6		2.750	0.391	26	56.3	4.7	22.1	16.9
2	2		1.795	0.397	19	11.8	88.2		
	3		2.357	0.391	34	0.0	100.0		
	4		2.373	0.397	41	15.8	62.1	22.0	
	5		3.042						
	6		2.517	0.397	19	17.5	52.6	19.9	9.9
4	4		1.843	0.391	34	33.5	2.8	63.7	
	5		2.543	0.391	34	0.0	11.5	88.5	
0	0		1.916	0.409	48	100.0			
	2		2.446	0.391	34	50.3	49.7		
0	0		2.190	0.180	46	100.0			
6	6		3.057	0.397	41	2.4	6.1	42.4	49.1

[a] Sakai, Ref. 41.

ent and at the shape at which the wave function maximum occurs.

Tables III–V give the calculated energies, (β,γ) values for the wave function maxima, and the % K components for the allowed K values. Experimental energies from the tables of Sakai,[41] and Endt and van der Leun[42] are also given. Contour plots of the calculated potential energy surfaces and two mass parameter functions are given in Figs. 8–12. Note that *no* theoretical parameter has been adjusted to fit the experimental spectra.

Although all the three nuclei considered here are well-deformed ($\beta=0.3$–0.4, $E_4/E_2=3.0$–3.3), there are some interesting differences. Of the three, the nucleus ^{102}Zr is closest to an ideal rotor, at least in the ground state band. The wave function maximum occurs for the same shape ($\beta=0.409$, $\gamma=12°$) for all four members of the ground state band. The K mixing is less than 2% for all four states (see Table III).

The above statement about the K mixing is valid also for ^{168}Er (see Table IV). However, the wave

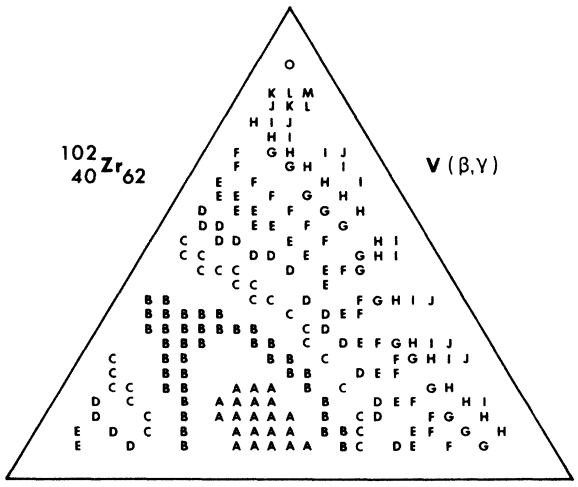

FIG. 8. Contour plot of the potential energy of ^{102}Zr. The symbols $A, B, \ldots, O$ refer to 0.0–0.7, 1.4–2.1, ..., 19.6–20.3 MeV. Deformation β varies radially from 0.0 to 0.8 and γ from 0° to 60° from the left corner of the triangle.

TABLE IV. Energy levels and wave functions of $^{168}_{68}Er_{100}$.

Most prob. K	I	Excitation energy (MeV) Ex.[a]	Th.	Wave function max. at β	γ (deg)	Calc. wave functions % K component $K=0$	$K=2$	$K=4$	$K=6$
0	0	0.0	0.0	0.312	16	100.0			
(g)	2	0.080	0.073	0.312	16	99.9	0.1		
	4	0.264	0.279	0.278	9	99.5	0.5	0.0	
	6	0.549	0.705	0.278	9	97.9	1.9	0.1	0.0
2	2	0.821	0.747	0.304	25	2.1	97.9		
(γ)	3	0.896	0.999	0.304	25	0.0	100.0		
	4	0.995	1.037	0.304	25	11.3	88.1	0.6	
	5	1.118	1.342	0.304	25	0.0	98.5	1.5	
	6	1.264	1.447	0.304	25	20.3	76.3	3.3	0.1
0	0	1.217	0.870	0.304	35	100.0			
(β)	2	1.277	1.024	0.304	35	97.5	2.5		
	4	1.411	1.399	0.391	34	87.8	11.3	0.9	
	6	1.617	1.951	0.260	30	73.2	24.9	1.7	0.3
4	4		1.545	0.304	25	1.3	1.5	97.2	
	5		1.886	0.260	30	0.0	4.4	95.6	
	6		2.056	0.304	25	6.7	6.0	84.5	2.8
2	2		1.639	0.312	44	7.7	92.3		
	3		2.101	0.350	38	0.0	100.0		
	4		1.990	0.350	38	9.9	79.3	10.8	
0	0		1.802	0.391	34	100.0			
	2		2.062	0.433	30	93.3	6.7		
6	6		2.401	0.391	34	5.5	18.0	11.6	64.8
0	0		1.950	0.278	51	100.0			

[a] Sakai, Ref. 41.

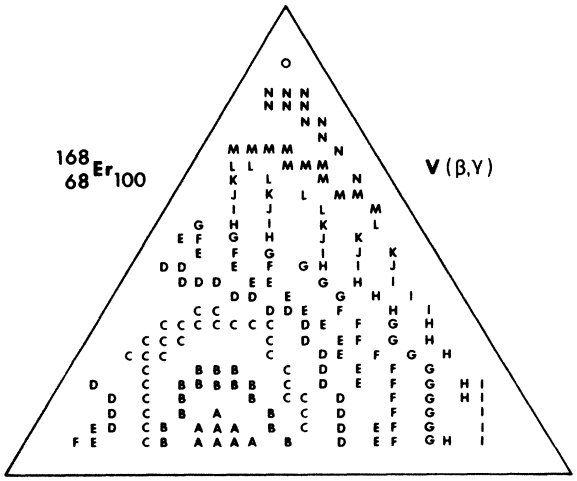

FIG. 9. Contour plot for the potential energy of ^{168}Er. The symbols $A, B, \ldots, O$ refer to 0.0–0.6, 1.2–1.8, ..., 16.8–17.4 MeV. See Fig. 8 caption for β, γ values.

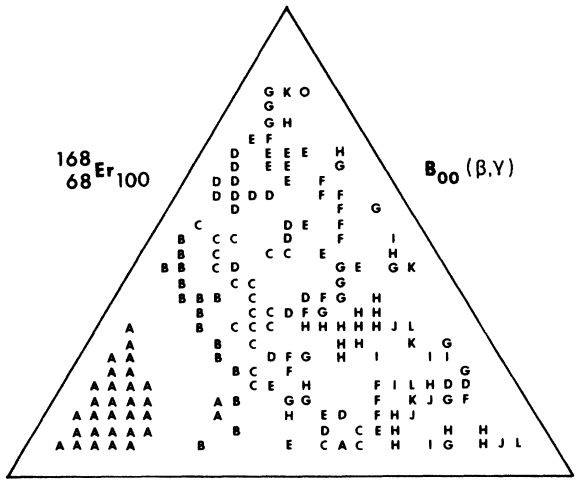

FIG. 10. Contour plot for the mass parameter function B_{00} of ^{168}Er. The symbols $A, B, \ldots, O$ refer to 0.35–0.94, 1.53–2.12, ..., 16.86–17.45 MeV^{-1}. See Fig. 8 caption for β, γ values.

TABLE V. Energy levels and wave functions of $^{24}_{12}Mg_{12}$.

Most prob. K	I	Excitation energy (MeV) Ex.[a,b]	Th.	Wave function max. at β	γ (deg)	Calc. wave functions % K components $K=0$	$K=2$	$K=4$	$K=6$
0	0	0.0	0.0	0.409	48	100.0			
	2	1.369	1.200	0.391	26	59.4	40.6		
	4	4.123	3.596	0.391	26	55.8	28.2	15.9	
	6	8.120	8.293	0.391	26	42.3	15.1	17.8	24.8
0	0		1.504	0.218	37	100.0			
	2		1.954	0.391	26	51.1	48.9		
	4		4.485	0.391	26	51.7	16.9	31.5	
	6		7.098	0.391	26	61.8	27.0	7.0	4.1
2	2	4.239	3.451	0.218	37	29.9	70.1		
	3	5.236	3.846	0.391	26	0.0	100.0		
	4	6.010	5.658	0.391	26	3.3	71.0	25.8	
	5	7.811	7.246	0.391	26	0.0	85.1	14.9	
	6	9.520	9.405	0.391	26	7.4	68.7	4.4	19.5
0	0		3.969	0.391	26	100.0			
	2		6.252	0.218	37	56.8	43.2		
	4		9.237	0.218	37	77.7	17.0	5.3	
0	0		4.941	0.606	52	100.0			
	2		5.081	0.409	48	60.9	39.1		
	4		7.036	0.409	48	36.1	35.4	28.5	
2	2		5.645	0.218	37	51.6	48.4		
	3		6.840	0.218	37	0.0	100.0		
0	0	6.432	6.883	0.776	3	100.0			
	2	7.348	8.060	0.776	3	93.6	6.4		
	4	8.436	10.257	0.776	3	58.2	23.6	18.3	
2	2	8.654	7.489	0.218	37	25.3	74.7		
	3	9.456	9.363	0.218	37	0.0	100.0		
0	0	8.85	8.237	0.687	49	100.0			
	2	10.36	9.847	0.661	41	75.2	24.8		
	4		11.064	0.776	3	54.1	39.8	6.2	
4	4	9.300	8.349	0.606	52	20.7	30.9	48.4	
	5		8.740	0.409	48	0.0	26.3	73.7	
4	4	9.515	9.610	0.391	26	17.5	4.9	77.6	
6	6		11.059	0.409	48	15.3	31.2	8.7	44.8

[a] Endt and van der Leun, Ref. 42.
[b] Sakai, Ref. 41.

function maximum shifts from (0.312, 16°) for $I=0,2$ to (0.278, 9°) for $I=4,6$.

Deviations from the ideal rotor are strongest in the case of ^{24}Mg. First we note that although the potential minimum occurs for an asymmetric shape on the prolate side ($\beta=0.44$, $\gamma=17°$), the dynamics shifts the ground state wave function maximum to an asymmetric shape on the oblate side (0.409, 48°). The nonaxiality is responsible for a 41% mixing of $K=2$ into the first excited 2^+ state. It is also interesting to note that while the calculated energy gap $\Delta(\Delta=\Delta_p=\Delta_n$ for this nucleus with $Z=N)$ is zero for shapes close to the potential minimum, it is as large as 1.9 MeV for some shapes. Hence, we believe that the pairing effects should not be neglected even for nuclei as light as ^{24}Mg.

On the other hand, the quasiparticle theory of pairing is probably not adequate for ^{24}Mg because errors due to particle number nonconservation are expected to be more serious for lighter nuclei. A consequence of this seems to be that we get a sharp peak in the calculated mass parameter function $B_{00}(\beta,\gamma)$ for ^{24}Mg at $\beta=0.218$, $\gamma=37°$ (see Fig. 12). (Note that there is no such peak in the

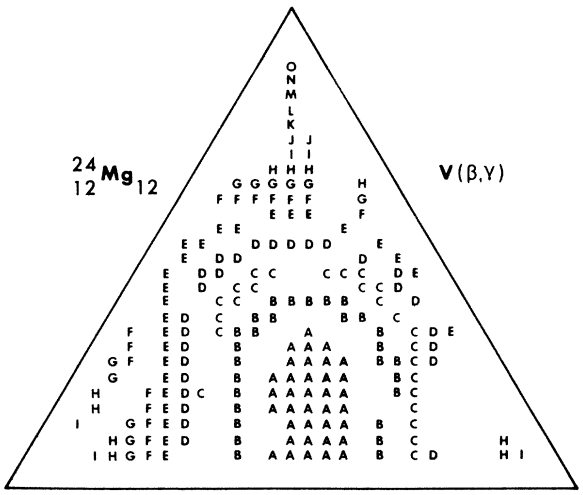

FIG. 11. Contour plot for the potential energy of ^{24}Mg. The symbols $A, B, \ldots, O$ refer to 0.0–0.43, 0.86–1.29, ..., 12.04–12.47 MeV. See Fig. 8 caption for the β, γ values.

case of ^{168}Er, see Fig. 10.) This creates an extra $K=0$ band starting at only 1.504 MeV (see Table V). Note that there is no indication of a second minimum in the potential energy in the neighborhood of $\beta=0.218$, $\gamma=37°$ (Fig. 11). This peculiar behavior of the calculated mass parameter may also be responsible for the other low-lying bands in Table V which have not been observed experimentally.

Figure 13 gives a comparison of the calculated moments of inertia with experiment for the three well-deformed nuclei discussed above, as well as for three transitional nuclei: ^{186,190,192}Os. The figure gives two types of moments of inertia. The static moment of inertia refers to the potential minimum (β_s, γ_s). Since this minimum is in general nonaxially symmetric, we define

$$\mathcal{I}_{\rm sta}=[2(\mathcal{I}_x^{-1}+\mathcal{I}_y^{-1})^{-1}]_{\beta=\beta_S,\gamma=\gamma_S}. \tag{70}$$

The dynamic moment of inertia is defined as

$$\mathcal{I}_{\rm dyn}=3/E_{2^+}, \tag{71}$$

where E_{2^+} is the excitation energy of the first 2^+ state. For an ideal, axially symmetric rotor, we would have $\mathcal{I}_{\rm dyn}=\mathcal{I}_{\rm sta}$. The experimental moment of inertia is deduced from the experimental E_{2^+} via Eq. (71). The calculated $\mathcal{I}_{\rm dyn}$ gives the correct A dependence of $\mathcal{I}$ over a wide range of A without any parameter adjustment. The magnitudes also agree with experiment within 16% in the case of the three well-deformed nuclei. But in the case of the three transitional nuclei, the calculated $\mathcal{I}_{\rm dyn}$ is too small (or, E_{2^+} is too large) by a factor of 1.2–1.9.

Since the factor of 1.2 in the case of ^{192}Os is comparable to the kind of agreement (or disagreement) obtained for the moments of inertia of the well-deformed nuclei, we give in Table VI a more detailed comparison with the experimental spectrum of ^{192}Os. The present calculation gives a reasonable energy for the first two 2^+ states. Also, the second 2^+ state is below the first 4^+ state in agree-

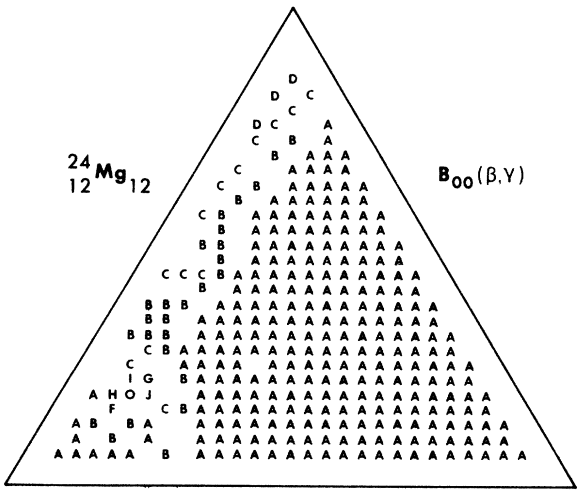

FIG. 12. Contour plot for the mass parameter function B_{00} of ^{24}Mg. The symbols $A, B, \ldots, O$ refer to 0.001–0.048, 0.096–0.143, ..., 1.327–1.374 MeV^{-1}. See Fig. 8 caption for the β, γ values.

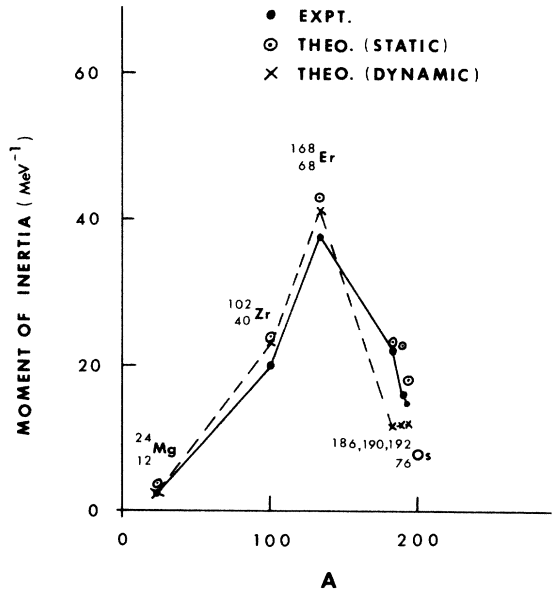

FIG. 13. Theoretical and experimental moments of inertia for selected nuclei. Both the experimental and the dynamical values correspond to $3/E_{2^+}$. The static values correspond to the calculated potential minimum.

TABLE VI. Energy levels and wave functions of $^{192}_{76}$Os.

Band	I	Excitation energy (MeV) Ex.[a]	Th.	Calc. wave functions: Wave function max. at β	γ (deg)	% K component $K=0$	$K=2$	$K=4$	$K=6$
g	0	0.0	0.0	0.218	37	100.0			
	2	0.206	0.252	0.218	37	67.2	32.8		
	4	0.580	0.744	0.218	37	56.9	35.2	7.9	
	6	1.089	1.410	0.218	37	47.8	36.9	12.5	2.8
γ	2	0.489	0.569	0.218	37	36.3	63.7		
	3	0.690	1.180	0.218	37	0.0	100.0		
	4	0.909	1.257[b]	0.218	23	44.3	16.9	38.8	
	5	1.143	1.875	0.218	37	0.0	67.9	32.1	
	6	1.362	2.032[b]	0.218	23	57.9	11.6	18.7	11.7
2γ	4	(1.069)	1.584	0.218	37	9.6	42.0	48.4	
	5		2.389	0.218	37	0.0	35.6	64.4	
	6	(1.465)	2.703						

[a] M. R. Schmorak, Nucl. Data Sheets 9, 195 (1973).

[b] Although the largest K component of the calculated wave function is for $K=0$, this level has been placed here since there is no lower $K=0$ band where it may be placed. The first excited 0^+ state (calculated) occurs at 1.741 MeV.

ment with experiment. However, the higher members of the ground and the γ-vibrational bands are too high by 0.2–0.7 MeV.

A possible reason for such large discrepancies is the neglect of the Villars-Cooper terms[13,14] which arise from replacing the quantization conditions $\omega_k = \hbar I_k / \mathcal{I}_k$ by $\omega_k = \hbar R_k / \mathcal{I}_k$, where $\vec{I}$ is total angular momentum while $\vec{R}$ is rotation of intrinsic axes with respect to the lab axes. The later condition would give additional terms, called rotation-particle-coupling and recoil terms,[10,36,43] in the collective Hamiltonian. These terms are expected to be small in the case of even-even nuclei if the deformation is large (which gives large $\mathcal{I}_k$) and if $\vec{I}$ is not very large. However, they become important at high spins and at small deformations.[43]

We do not give a comparison with other theoretical calculations for these nuclei because we are not claiming to present here the "best" theory of these nuclei. As pointed out in the Introduction, we have performed these calculations to answer the question: Is our DQP basis good enough for predicting the low-energy spectra of even-even nuclei without any adjustment of parameters from nucleus to nucleus? Our conclusions are given in the next section.

VI. CONCLUSIONS AND SUGGESTIONS FOR FUTURE IMPROVEMENTS

Our main conclusion is that the DQP basis discussed in this paper is good enough for studying the low-energy spectra of even-even nuclei. By this we do not mean that we have found a perfectly satisfactory model or theory. In order to clarify these seemingly contradictory statements, we first summarize the main virtues and limitations of the theory discussed above.

We have parametrized the Nilsson model Hamiltonian in such a way that the model parameters are independent of Z and A, except for an overall scaling factor for the Hamiltonian and the energy levels. The calculated single-particle wave functions are independent of Z and A, and are the same for protons and neutrons.

This single-particle basis is combined with an improved theory of pairing where the particle-hole matrix elements of the pairing force are treated as well as the particle-particle matrix elements. In this improved theory, a long standing problem of an occasional divergence in the calculation of rotational moments of inertia and vibrational mass parameters is removed.

The combined deformed-quasiparticle basis is employed to calculate the potential energy functions of ^{148,150,152,154}Sm, ^{186,188,190,192,194}Os, and ^{184,186,188,190}Hg, and the low-energy spectra of ^{102}Zr, ^{168}Er, and ^{24}Mg. Without *any* adjustment of model parameters, and using the *same* single-particle wave functions for all these nuclei (and many more, not reported here for the sake of brevity), we get the expected features: spherical-deformed transition at $N=88-90$, prolate-oblate transition in the Os region, shape as well as gap transitions in

the Hg nuclei.

Furthermore, good agreement is obtained with the energies of the rotational bands of deformed nuclei of three different mass regions (^{102}Zr, ^{168}Er, and ^{24}Mg), again without any adjustment of parameters.

Now, what are the limitations of the present calculation? First, the present discussion has been limited to the energy levels alone. However, this is not a serious limitation. Theory and codes for the calculation of electromagnetic moments exist already. Such calculations must be presented in future reports of the present program.

Secondly, the present basis is not large enough for the calculation of fission barriers and the spectra of well-deformed nuclei with $A > 208$. Previous experience suggests that one needs to include up to $\mathfrak{N} = 10$ shells, while we go up to $\mathfrak{N} = 8$ only. Before going to a larger basis, we decided to first test the present theory in a smaller basis.

Thirdly, the present calculation for ^{24}Mg has given some bands which are too low compared with experiment. A possible reason for this has been discussed in Sec. V. But this question certainly requires further studies.

Fourthly, the present calculation of the spectra is limited to well-deformed nuclei. Preliminary calculations for some transitional nuclei gave excitation energies which were too high compared with experiment. We could have presented reasonable fits to the spectra of such nuclei also, if we had allowed ourselves to introduce some arbitrary parameters to renormalize the potential and inertial functions. In our previous calculations, based on the pairing-plus-quadrupole force model, we did use one free parameter for the potential energy and one for the inertial functions. But we had the excuse that the configuration space was too small, which we do not have anymore.

Recently, Rohozinsky *et al.*[15] have performed large basis, dynamic calculations for several transitional nuclei. They also had the problems discussed above. Hence, they decided to introduce three arbitrary parameters—two for the potential energy and one for the inertial functions of each nucleus.

Further improvements in the present theory can probably be made by including the rotation-particle-coupling terms mentioned in Sec. V. Note that the inclusion of these terms does not require an additional parameter. These terms will certainly increase the complications of our computations. But this is where our DQP basis presents the best advantages.

The computation of the six million matrix elements of the deformed basis required 8 hours of UNIVAC 1110 at Orsay. However, the same matrix elements (stored on tapes) are employed for different nuclei. Hence, the UNIVAC 1110 time for computation of the potential function $V(\beta, 0)$, i.e., the static part of the calculation, is only 5 min/nucleus. Computation time for the dynamic part of the calculation is 20 min/nucleus (15 minutes for the β-γ-dependent potential and inertial functions, and 5 minutes for the calculation of about 20 nuclear states).

The calculations presented above include the leading order terms in nucleon-nucleus (particle-collective) coupling. True, we have not employed any terms which exhibit explicitly any nucleon-nucleus coupling. But the two types of motion are certainly coupled. The nucleon motion is governed by the nuclear shape. The dynamics of collective nuclear motion determines the most probable shape for each nuclear state.

ACKNOWLEDGMENTS

We are grateful to Dr. H. C. Pauli and to Dr. S. Rohozinski for discussions and for communicating their results prior to publication. We thank for their expert help the computer center personnel at Institut de Physique Nucléaire (Orsay), at Vanderbilt University (Nashville), and at Emory University (Atlanta).

APPENDIX I. MULTIPOLE EXPANSION OF NUCLEAR SURFACE

In the Hill-Wheeler parameterization of nuclear deformations, the semiaxis lengths of an ellipsoid are defined via Eq. (4), which may be rewritten as (all lengths are expressed below in units of R_0)

$$a = R_1/R_0 = \exp[-\delta \cos(\gamma + 60^\circ)], \tag{A1}$$

$$b = R_2/R_0 = \exp[-\delta \cos(\gamma - 60^\circ)], \tag{A2}$$

$$c = R_3/R_0 = \exp[\delta \cos\gamma]. \tag{A3}$$

The radius vector of a point (R, θ, ϕ) on the surface of the nuclear ellipsoid is given by

$$R(\theta, \phi) = \left(\frac{\sin^2\theta \cos^2\phi}{a^2} + \frac{\sin^2\theta \sin^2\phi}{b^2} + \frac{\cos^2\theta}{c^2}\right)^{-1/2}. \tag{A4}$$

A spherical multipole expansion of the surface is given by

$$R(\theta, \phi) = \sum_{\lambda\mu} a_{\lambda\mu} Y_{\lambda\mu}(\theta, \phi). \tag{A5}$$

For the ellipsoid surface defined by Eq. (A4), we have the symmetry conditions

$$R(\theta, \phi) = R(\theta, \phi + \pi), \tag{A6}$$

and

TABLE VII. Spherical multipole expansion coefficients for the surface of a Hill-Wheeler Ellipsoid. The deformation parameter β equals $(4\pi/5)^{1/2}\delta$. The parameter γ equals 0° or 60° (starred β values).

β	a_{00}	a_{20}	a_{22}	a_{40}	a_{42}	a_{44}
0.8*	3.368	0.378	0.464	0.079	0.084	0.111
0.7*	3.408	0.336	0.412	0.062	0.065	0.087
0.6*	3.444	0.292	0.358	0.046	0.049	0.065
0.5*	3.474	0.246	0.302	0.032	0.034	0.046
0.4*	3.499	0.199	0.243	0.021	0.022	0.030
0.3*	3.519	0.150	0.183	0.012	0.012	0.016
0.2*	3.533	0.100	0.122	0.005	0.005	0.007
0.1*	3.542	0.050	0.061	0.001	0.001	0.001
0	3.544	0	0	0	0	0
0.1	3.542	0.099	0	0.003	0	0
0.2	3.533	0.197	0	0.014	0	0
0.3	3.519	0.292	0	0.031	0	0
0.4	3.500	0.384	0	0.054	0	0
0.5	3.476	0.471	0	0.083	0	0
0.6	3.447	0.555	0	0.116	0	0
0.7	3.414	0.633	0	0.154	0	0
0.8	3.376	0.707	0	0.195	0	0

$$R(\theta,\phi)=R(\pi-\theta,\phi). \tag{A7}$$

The condition (A7) leads to the restriction

$$a_{\lambda\mu}=0 \quad \text{for } \lambda=\text{odd}. \tag{A8}$$

The condition (A6) leads to the restrictions

$$a_{\lambda\mu}=0 \quad \text{for } \mu=\text{odd}, \tag{A9}$$

$$a_{\lambda\mu}=a_{\lambda,-\mu} \quad \text{for } \mu=\text{even}. \tag{A10}$$

The coefficients $a_{\lambda\mu}$ for $\lambda=0,2,4$ are given, up to second order in δ, by

$$a_{00}=(4\pi)^{1/2}(1-\delta^2/5), \tag{A11}$$

$$a_{20}=(4\pi/5)^{1/2}[\delta\cos\gamma-(1/14)\delta^2\cos2\gamma], \tag{A12}$$

$$a_{22}=(2\pi/5)^{1/2}[\delta\sin\gamma+(1/14)\delta^2\sin2\gamma], \tag{A13}$$

$$a_{40}=(4\pi)^{1/2}(3/70)\delta^2(5\cos^2\gamma+1), \tag{A14}$$

$$a_{42}=(30\pi)^{1/2}(3/70)\delta^2\sin2\gamma, \tag{A15}$$

$$a_{44}=(70\pi)^{1/2}(3/70)\delta^2\sin^2\gamma. \tag{A16}$$

Those for $\lambda=0,2$ were given previously by Carlson.[46] Exact, numerical values of $a_{\lambda\mu}$ can be computed with the Gauss-Legendre method. Such values are given in Table VII for some axially symmetric shapes. Table VII shows that the Hill-Wheeler parameterization induces some non-negligible hexadecapole ($\lambda=4$) deformations.

APPENDIX II. COULOMB, SURFACE, AND CURVATURE FUNCTIONS OF DEFORMATION

Because of the symmetries of the ellipsoid, we can order the semiaxis lengths such that

$$a\geq b\geq c, \tag{A17}$$

and define the eccentricities

$$\epsilon=(1-c^2/a^2)^{1/2}, \tag{A18}$$

$$\epsilon'=(1-b^2/a^2)^{1/2}\leq\epsilon, \tag{A19}$$

$$\epsilon''=(1-c^2/b^2)^{1/2}. \tag{A20}$$

The Coulomb function B_C is defined by the ratio of the Coulomb energy of the ellipsoid to the energy of the sphere. Assuming that the surfaces of constant charge density are a family of similar concentric ellipsoids, the Coulomb energy is given by[46]

$$U(a,b,c)=\langle R^2(\theta,\phi)\rangle U(1,1,1), \tag{A21}$$

where $R(\theta,\phi)$ is the radius vector of a point on the surface of the ellipsoid. With the definition given above, we have

$$B_C=\langle R^2(\theta,\phi)\rangle=(4\pi)^{-1}\int_0^{2\pi}\int_0^{\pi}R^2(\theta,\phi)\sin\theta d\theta d\phi. \tag{A22}$$

As shown by Carlson,[46] the integral (A22) can be rewritten as

$$B_C=(a\epsilon)^{-1}F(\psi,k), \tag{A23}$$

where $F(\psi,k)$ is the incomplete elliptical integral of the first kind with

$$\sin\psi=\epsilon, \tag{A24}$$

and

$$k=\epsilon'/\epsilon. \tag{A25}$$

The surface function B_s is defined as the ratio of the ellipsoid area S to the sphere area. The quantity S is given by Jordan[47] to be

$$S=2\pi ab\{(1/\epsilon-\epsilon)F(\psi,k')+\epsilon E(\psi,k')+[(1-\epsilon^2)(1-\epsilon''^2)]^{1/2}\}, \tag{A26}$$

where $E(\psi,k')$ is the incomplete elliptical integral of the second kind, ψ is defined by Eq. (A24), and

$$k'=\epsilon''/\epsilon. \tag{A27}$$

Using Eq. (A26) and the condition $abc=1$, we get

$$B_s=\frac{S}{4\pi}=\frac{1}{2c}\{(1/\epsilon-\epsilon)F(\psi,k')+\epsilon E(\psi,k')+[(1-\epsilon^2)(1-\epsilon''^2)]^{1/2}\}. \tag{A28}$$

The curvature function B_k is given for axially symmetric shapes by Seeger and Howard.[26] Their table shows that at least for such shapes, the function

$$B_k\approx B_s. \tag{A29}$$

Since the coefficient of the B_k term of the liquid drop energy [see Eq. (60) of the text] is quite small, we assume that Eq. (A29) is valid for all deformations considered in the present calculations.

*Work at Vanderbilt University supported partially by U. S. Energy Research and Development Administration.

†Part of this work was carried out while this author was a summer visitor at Institut de Physique Nucléaire, Orsay.

‡Part of this work was carried out while this author was on leave at Vanderbilt University.

[1]V. M. Strutinsky, Yad. Fiz. 3, 614 (1966) [Sov. J. Nucl. Phys. 3, 449].

[2]J. R. Nix, Annu. Rev. Nucl. Sci. 22, 65 (1972).

[3]M. Baranger, in *Proceedings of the International Conference on Nuclear Physics, Munich*, 1973, edited by J. de Boer and H. J. Mang (North-Holland, Amsterdam/American Elsevier, New York, 1973), Vol. 2, p. 93.

[4]M. Brack and P. Quentin, Phys. Lett. 56B, 421 (1975).

[5]A. Bohr, K. Dan. Vidensk. Selsk. Mat. Fys. Medd. 26, No. 14 (1952).

[6]K. Kumar, *A Study of Nuclear Deformations with Pairing Plus Quadrupole Forces*, Ph.D. thesis (unpublished), available from Carnegie-Hunt Library, Pittsburgh.

[7]K. Kumar and M. Baranger, Nucl. Phys. A122, 273 (1968).

[8]S. G. Nilsson, K. Dan. Vidensk. Selsk. Mat.-Fys. Medd. 29, No. 16 (1955).

[9]D. L. Hill and J. A. Wheeler, Phys. Rev. 89, 1102 (1953).

[10]A. Bohr and B. R. Mottelson, *Nuclear Structure* (Benjamin, New York, 1969), Vol. 1; *Nuclear Structure* (Benjamin, New York, 1975), Vol. 2.

[11]Y. Yariv, T. Ledergerber, and H. C. Pauli, Z. Phys. A278, 225 (1976).

[12]K. Kumar, Nucl. Phys. A231, 189 (1974).

[13]F. M. H. Villars and G. Cooper, Ann. Phys. (N.Y.) 56, 224 (1970).

[14]A. de-Shalit and H. Feshbach, *Theoretical Nuclear Physics* (Wiley, New York, 1974).

[15]J. Dobaczewski, S. G. Rohozinski, and J. Srebrny, Nukleonika 20, 981 (1975); T. Kaniowska, A. Sobiczewski, K. Pomorski, and S. G. Rohozinski, Nucl. Phys. A274, 151 (1976).

[16]C. Gustafson, I. L. Lamm, B. Nilsson, and S. G. Nilsson, Ark. Fys. 36, 613 (1967).

[17]K. Kumar, Phys. Rev. C 1, 369 (1970).

[18]Some recent Nilsson model calculations also take into account the γ degree of freedom. See, e.g., Ref. 15.

[19]M. Baranger and K. Kumar, Nucl. Phys. A110, 490 (1968).

[20]This type of argument had led us previously (see Ref. 19) to propose the use of different b values for protons and neutrons (keeping $\hbar\omega_0$ the same for both), and to introduce the factors α_p, α_n. These factors are not needed in the present formulation.

[21]R. V. Gentry *et al.*, Phys. Rev. Lett. 37, 11 (1976); C. J. Sparks, Jr., *ibid.* 38, 205 (1977).

[22]K. Kumar, Nukleonika 20, 133 (1975).

[23]N. N. Bogolyubov, Nuovo Cimento 7, 794 (1958).

[24]L. Grodzins, Annu. Rev. Nucl. Sci. 18, 291 (1968), Table II.

[25]M. Born and J. R. Oppenheimer, Ann. Phys. (Leipzig) 84, 457 (1927).

[26]P. A. Seeger and W. M. Howard, Nucl. Phys. A238, 491 (1975).

[27]J. Bonn *et al.*, Phys. Lett. 38B, 308 (1972); Z. Phys. A276, 203 (1976).

[28]R. Foucher, Rapports Internes, Institut de Physique Nucléaire, No. 9, 1971 and No. 2, 1973 (unpublished); C. Bourgeois *et al.*, J. de Phys. 37, 49 (1976).

[29]J. H. Hamilton *et al.*, Phys. Rev. Lett. 35, 562 (1975).

[30]J. D. Cole *et al.*, Phys. Rev. Lett. 37, 1185 (1976).

[31]K. Kumar and B. Sørensen, Nucl. Phys. A146, 1 (1970).

[32]K. Kumar, Bull. Am. Phys. Soc. 20, 736 (1975); 21, 613 (1976).

[33]D. Vautherin, in *Proceedings of the International Conference on Nuclear Physics, Munich, 1976* (see Ref. 3), Vol. 2, p. 107.

[34]D. Gogny, in *Nuclear Self-Consistent Fields*, proceedings of the International Conference held at the International Center for Theoretical Physics, Trieste, Italy, 1975, edited by G. Ripka and M. Porneuf (North-Holland, Amsterdam, 1975), p. 333.

[35]D. R. Inglis, Phys. Rev. 97, 701 (1955).

[36]A. K. Kerman, in *Nuclear Reactions* (North-Holland, Amsterdam, 1959), Vol. 1, p. 427; Ann. Phys. (N.Y.) 12, 300 (1961).

[37]D. R. Bès, K. Dan. Vidensk. Selsk. Mat.-Fys. Medd. 33, No. 2 (1961).

[38]M. Baranger and K. Kumar, Nucl. Phys. A122, 241 (1968).

[39]K. Kumar and M. Baranger, Nucl. Phys. A92, 608 (1967).

[40]K. Kumar, in *The Electromagnetic Interaction in Nuclear Spectroscopy*, edited by W. D. Hamilton (North-Holland, Amsterdam, 1975), p. 55.

[41]M. Sakai, Nucl. Data Tables 15, 513 (1975).

[42]P. M. Endt and C. van der Leun, Nucl. Phys. A214, 1 (1973).

[43]F. S. Stephens and R. S. Simon, Nucl. Phys. A183, 257 (1972).

[44]M. A. Preston and R. K. Bhaduri, *Structure of the Nucleus* (Addison-Wesley, Reading, 1975), pp. 395–403.

[45]S. T. Belyaev, Nucl. Phys. 64, 17 (1965).

[46]B. C. Carlson, J. Math. Phys. 2, 441 (1961).

[47]C. Jordan, *Cours d'analyse* (Gauthier-Villars, Paris, 1959).

[48]J. B. Gupta, K. Kumar, and J. H. Hamilton, Phys. Rev. C 16, 427 (1977).

[49]T. Kishimoto and T. Tamura, Nucl. Phys. A270, 317 (1976).

[50]A. Faessler *et al.*, Phys. Lett. 48B, 87 (1974).